

THE ELASTIC PROPERTIES AND LATTICE DYNAMICS FOR SELECTED 211 MAX PHASES: A DFT STUDY

A PREPRINT

G. K. Arusei^{*1}, M. Chepkoech², G. O. Amolo³, and N. Makau⁴

^{1,4}Department of Physics, University of Eldoret, P.O Box 1125, Eldoret (Kenya)

²University of Kabianga (UoK), P.O.Box 2030, 20200 Kericho, Kenya

³School of Physics and Earth Sciences, The Technical University of Kenya, P.O. Box 52428-00200, Nairobi, Kenya

^{*}Email id: aruseig@yahoo.com

ABSTRACT

The elastic properties and lattice dynamics of Ti_2AlC , Ti_2AlN , Ti_2GaC , Ti_2GaN , Ti_2PbC , Ti_2CdC and Ti_2SnC have been investigated using the density functional theory within the generalized gradient approximations as expressed in Quantum Espresso and VASP codes. The obtained lattice parameters are in agreement with the previous theoretical research and available experimental data. The elastic properties of the MAX phases under study have been calculated. The values of elastic anisotropy, Young's modulus, Poisson ratio and shear modulus reveal that the compounds are stable and ductile and that Ti_2PbC and Ti_2CdC are more stable than the other considered compounds. Thus, the seven compounds may be useful for industrial applications. The calculated phonon spectra confirm that the studied MAX phases are dynamically stable because of the absence of imaginary phonon modes. The temperature dependent lattice thermal conductivity of MAX phases have been determined using the Debye theory as outlined by Slack. The obtained κ_{ph} for Ti_2AlC at 1300 K agree with experimental findings within 9%. The estimated minimum thermal conductivities (κ_{min}) of the MAX phases obtained by using empirical formula suggested by Clarke show that Ti_2PbC possesses the lowest minimum thermal conductivity.

Keywords MAX phases · Elastic constants · Phonon transport · Thermal conductivity

1 Introduction

MAX phases materials presented in this paper (Ti_2AlC , Ti_2AlN , Ti_2GaC , Ti_2GaN , Ti_2PbC , Ti_2CdC and Ti_2SnC) are ternary carbides and nitrides materials with the general formula $\text{M}_{n+1}\text{X}_n(\text{MAX})$ where $n = 1$, M is an early transition metal, A is an A-group element (mostly IIIA and IVA) and X is either C or N-represent a new class of thermodynamically stable nano-laminated solids [1] with unique combination of ceramic and metallic properties. The $\text{M}_{n+1}\text{AX}_n$ phases crystallize in the hexagonal structure belonging to the space group of P63/mmc. MAX phases mimic ceramics in that they are stiff, resistant to oxidation, and remain strong at temperatures beyond 1400C. The metal-like properties of MAX phases manifest themselves in their machinability, resistance to thermal shock, high damage tolerance, and electrical and thermal conductivity [1, 2]. These unique combination of properties suits as structural materials for demanding environmental operations like increasing the efficiency of engines requires operation at much higher temperatures than what is allowed by today's materials.

Up to now, lack of large MAX single crystals has made it very hard to determine experimentally the elastic constants of these compounds. However, the ab initio results are available. Research efforts have been made to study the physical properties of M_2AX phases both theoretically and experimentally [3, 4, 5, 6, 7, 8, 9, 10, 11, 12] and a few of these materials have been fully investigated. Among the compounds, there are few studies on technological importance on M_2InC (M = Zr, Hf and Ta) MAX phases [11, 13, 14, 15, 16, 17].

A lot of work has been carried out with Al as an A element and C as X element in MAX-series [18, 19, 20]. Moreover, the structural, electronic and elastic properties of $M_2\text{GaN}$ compounds have been done by Bouhemadou [21]. Dhakal et al. [19] have also calculated the lattice thermal conductivity of 551 MAX phase compounds using the Debye theory as outlined by Slack model [22].

Theoretical calculations on the mechanical properties, lattice dynamics and thermal conductivity of the 211 MAX phases under study are limited and thus in this work, first principle density functional theory calculations will be done to examine the elastic properties of the selected materials with the aim of identifying optimum compositions that combine desirable machinability with high stiffness. In addition, the phonons and approximated thermal conductivity studies will be performed on these compounds and compared with the available theoretical and experimental data.

2 Computational details

The structural and mechanical properties of the MAX phases under study were determined by using density functional theory [23, 24] as implemented in the Quantum Espresso (QE) [25, 26, 27] and VASP [28] codes. The exchange-correlation functional is approximated using the Generalized Gradient Approximation (GGA) as proposed by Perdew, Burke and Ernzerhof [29]. The core electrons were described by the projector augmented wave method (PAW) [30, 31] (in VASP) and ultrasoft pseudopotentials [32] (in QE). A plane-wave kinetic cut-off energies of 60 Ry (for Ti_2SnC), 50 Ry (for Ti_2AlC , Ti_2AlN , Ti_2GaC and Ti_2GaN), 40 Ry (for Ti_2PbC) and 30 Ry (for Ti_2CdC) were determined through a careful convergence scheme. In VASP code, a kinetic cut-off of 520 eV was used to expand the electronic wave functions. The first Brillouin zone was sampled using a $12 \times 12 \times 10$ Monkhorst-Pack k-point grid [33].

In order to obtain reliable results, a highly accurate computational method, THERMO-PW method [34] was employed in this study to calculate the elastic constants as implemented in the QE code using the three accepted elastic stability for selected MAX Phases in this study [35, 34]. This method has proven successful in theoretical studies of elastic properties on various materials [35, 34]. In the case of VASP code, the elastic constants were calculated by the efficient stress-strain method [36]. The Phonopy code [37] was used to calculate the lattice dynamics of the MAX phases at the level of Harmonic approximations by using the finite displacement method. The second-order harmonic force constant were computed using a $2 \times 2 \times 2$ supercells consisting of 64 atoms. The temperature dependent lattice phonon thermal conductivity of MAX phases are determined using Slack's equation [22].

3 Results and discussions

3.1 Structural properties

$M_2\text{AX}$ crystallizes in hexagonal structure with the space group $P63mmc$ no. 194. The unit cell structure of $M_2\text{AX}$ compounds is depicted in Fig. 1. The unit cell composes of 2 formula units with 8 atoms. The equilibrium lattice parameters, such as the lattice constants and equilibrium cell volume of the MAX phases are calculated and are tabulated in Table 1. Our calculated results are compared with other reported results and available experimental data as listed in Table 1. The obtained lattice parameters are in good agreement with other theoretical data as listed in Table 1. The calculated lattice constants deviate from the experimental data by less than 2%.

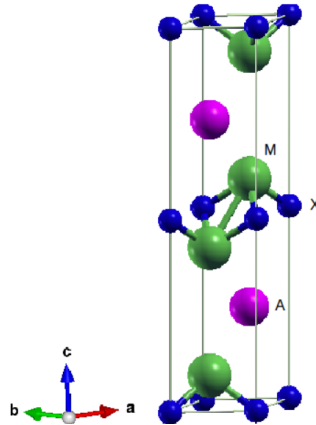


Figure 1: Crystal structure of the $M_2\text{AX}$ phase.

Table 1: The calculated equilibrium lattice parameters, a and c , (in Å), equilibrium cell volume, V_0 , (in Å³) of considered MAX phases obtained using VASP and QE codes compared with available theoretical and experimental data.

	a	b	V_0	Reference
Ti ₂ AlN	2.99 - 3.07	13.51 - 13.65	106 - 110.16	This Calc.
	2.961	13.652	106	[21]
	2.989	13.614	105.33	[38]
	2.98	13.68	105.21	Expt. [39]
	3.01	13.70	107.49	[39]
Ti ₂ AlC	3.07 - 3.10	13.74 - 13.82	115.57 - 112.08	This Calc.
	3.051	13.637	109.93	[38]
	3.04	13.59	108.77	Expt. [39]
	3.08	13.77	113.13	[39]
Ti ₂ GaC	3.07 - 3.08	13.46 - 13.51	110.16 - 110.56	This Calc.
	3.07	13.52	110.35	[38]
Ti ₂ GaN	3.02 - 3.07	3.352 - 13.51	105.12 - 110.16	This Calc.
	2.961	13.021	98.87	LDA [21]
	3.018	13.318	105.07	GGA [21]
	3.00	13.3	103.7	Expt. [15]
Ti ₂ SnC	3.18	13.80 - 13.97	120.48 - 121.96	This Calc.
	3.163	13.679	118.52	[38]
	3.1626	13.679	-	Expt. [40]
	3.164	13.675	-	Expt. [41]
	3.186	13.63	-	Expt. [42]
Ti ₂ CdC	3.07 - 3.11	14.118 - 14.53	115.16 - 121.36	This Calc.
	3.1	14.41	10119.92	[38]
	3.099	14.41	119.85	Expt. [43]
Ti ₂ PbC	3.23 - 3.28	13.78 - 14.01	126.48 - 128.47	This Calc.
	3.20	13.81	122.46	[38]
	3.222	13.99	125.78	Expt. [43]
	3.201	13.78	122.28	Expt. [44]

3.2 Mechanical properties

The mechanical behavior of solids depends upon their elastic constants. The elastic constants provide information on the stability, stiffness, brittleness, ductility, and elastic anisotropy of a given material. The MAX phases possess hexagonal crystal structures [38, 45] and thus have six elastic constants: C_{11} , C_{12} , C_{13} , C_{33} , C_{44} and C_{66} . The first five are independent elastic constants whereas the last one takes into account: $C_{66} = (C_{11} - C_{12})/2$.

A mechanically stable MAX compound should obey the following stability conditions [46, 47, 48]:

$$C_{11} > 0, C_{33} > 0, C_{44} > 0, (C_{12} - C_{12}) > 0, \text{ and} \\ (C_{11} + C_{12})C_{33} > 2(C_{12})^2.$$

The predicted elastic properties for considered materials MAX phases are tabulated in Table 3 together with the available theoretical data [18, 20, 49, 50, 51, 52]. From Table 2, it can be seen that our estimated elastic constants obey the above mentioned Born stability conditions [46, 47, 48] and thus confirms the studied MAX compounds are mechanically stable. Our calculated elastic constants for studied MAX phases are consistent with reported theoretical data [18, 20, 49, 50, 51, 52].

For all the materials $C_{33} > C_{11}$ (see Table 2), implying that the compounds are more incompressible along the c -direction than along the a -direction. It also indicates that the compounds are elastically anisotropic.

The elastic modulus (B , G , E , and ν) have been calculated from the elastic constants, C_{ij} using the Voigt-Reuss-Hill formula [53] and listed in Table 3. The bulk modulus provides a measure of resistance to volume change and the average bond strength in a material. The higher the bulk modulus the greater the bond strength. It is evident that Ti₂CdC possesses a smaller value of bulk modulus than those of other considered materials, and thus it possesses the lowest bond strength. Shear modulus plays a dominant role in predicting the hardness rather than bulk modulus. From Table 3

the shear modulus of Ti_2AlN is found to be higher than those of other materials under study, and as result, it is expected that Ti_2AlN should be harder compared to the other compounds.

Table 2: Calculated elastic constants C_{ij} (Gpa) for Ti_2AlC , Ti_2AlN , Ti_2GaC , Ti_2GaN , Ti_2PbC , Ti_2CdC and Ti_2SnC MAX phases obtained using VASP and QE codes compared with available theoretical and experimental data.

	C_{11}	C_{12}	C_{13}	C_{33}	C_{44}	A	Reference
Ti_2AlN	272.1 - 308.4	56.8 - 75.3	86.9 - 89.5	271.3 - 287.2	121.1 - 118.6	1.14 - 1.26	This Calc.
	342	56	96	283	123	1.14	[20]
	309	66	91	280	125	1.23	[18]
Ti_2AlC	274.7 - 297.3	50.4 - 63.6	49.3 - 59	246.8 - 262	101.7 - 110	0.96 - 0.98	This Calc.
	301	59	55	278	113	0.96	[49]
	302	62	61	269	109	0.97	[18]
Ti_2GaC	275.9 - 306.4	59.5 - 65.6	46.5 - 60.6	225.5 - 265.9	89.8 - 114	0.88 - 1.01	This Calc.
	314	66	59	272	122	1.04	[51]
Ti_2GaN	267.9 - 293	70.3 - 89.9	85.4 - 91.6	249.5 - 272.9	107.5 - 113	1.18 - 1.24	This Calc.
	338 \pm 2	97 \pm 2	111 \pm 0.8	312 \pm 3	136 \pm 1	1.27	LDA[21]
	296 \pm 1	84 \pm 0.7	92 \pm 0.4	275 \pm 3	119 \pm 0.5	1.23	GGA[21]
Ti_2SnC	228.0 - 265.5	74.2 - 78.2	47.7 - 71.2	202.7 - 263	74.0 - 91	0.88 - 0.94	This Calc.
	260	78	70	254	93	0.99	[50]
Ti_2CdC	226.5 - 251.1	59.2 - 73.2	43.8 - 44.9	183.6 - 203.6	29.8 - 79.4	0.33 - 0.98	This Calc.
	258	68	46	205	33	0.36	[52]
Ti_2PbC	202.5 - 239.1	81.9 - 90.6	49.7 - 51.4	195.7 - 213.2	60.8 - 65.1	0.75 - 0.81	This Calc.
	235	90	53	211	66	0.78	[50]

Table 3: Calculated elastic moduli B , G , E (Gpa) and ν for Ti_2AlC , Ti_2AlN , Ti_2GaC , Ti_2GaN , Ti_2PbC , Ti_2CdC and Ti_2SnC MAX phases obtained using VASP and QE codes compared with available theoretical and experimental data.

	B	G	E	B/C_{44}	B/G	ν	Reference
Ti_2AlN	141.7 - 155.1	108.2 - 126	258.6 - 277.3	1.17 - 1.31	1.23 - 1.31	0.19 - 0.2	This Calc.
	162.55	126	300	1.32	1.29	0.192	[20]
	177	127	307	1.42	1.39	-	[18]
Ti_2AlC	121.4 - 136.1	106.1 - 115	246.5 - 267	1.19 - 1.24	1.14 - 1.18	0.16 - 0.17	This Calc.
	135.33	118	277	1.20	1.15	0.164	[49]
	138	113	267	1.27	1.22	-	[18]
Ti_2GaC	140.8 - 153.6	98.6 - 108.2	239.8 - 263.5	1.31 - 1.35	1.42 - 1.43	0.17 - 0.22	This Calc.
	140.88	121	283	1.20	1.16	0.166	[51]
Ti_2GaN	119.5 - 138.8	98.8 - 110.5	232.3 - 262	1.23 - 1.33	1.21 - 1.26	0.18 - 0.19	This Calc.
	181	122	300	1.33	1.48	0.22	LDA [21]
	156	108	264	1.44	1.32	0.218	GGA [21]
Ti_2SnC	110.3 - 137.2	77.4 - 93	188.2 - 228	1.49 - 1.51	1.42 - 1.48	0.22	This Calc.
	134.44	93	226	1.45	1.45	0.218	[50]
Ti_2CdC	102.6 - 113.5	61.5 - 65	148.2 - 153.6	2.57 - 3.81	1.67 - 1.75	0.24 - 0.25	This Calc.
	115.66	69.6	174	3.51	1.66	0.249	[52]
Ti_2PbC	106.7 - 118.9	63.9 - 74	159.8 - 183.9	1.75 - 1.83	1.61 - 1.67	0.24 - 0.25	This Calc.
	119.22	73.2	182	1.81	1.63	0.245	[50]

Young's modulus (E) is used to measure of stiffness of a material, i.e., the larger the value of E , the stiffer the material and vice versa. The E values of the materials under study decrease in the order: $\text{Ti}_2\text{AlN} > \text{Ti}_2\text{AlC} > \text{Ti}_2\text{GaN} > \text{Ti}_2\text{GaC} > \text{Ti}_2\text{SnC} > \text{Ti}_2\text{PbC} > \text{Ti}_2\text{CdC}$. Thus, Ti_2AlN is stiffest (see Table 3).

Poisson's ratio plays another important role in assessing the nature of chemical bonding in solid materials [54]. The values of Poisson's ratio for pure covalent and ionic crystal are respectively, 0.1 and 0.25. The Poisson's ratio for the studied materials lies between these two characteristic values, indicating that the compounds possess mixture of covalent and ionic bonding.

The elastic anisotropy factor A determines how the elastic properties of a solid are dependent on the direction of the stress. Moreover, the elastic anisotropy is connected with the thermal expansion and the crystal micro-cracks

[55]. For the MAX phase systems that are hexagonal, the elastic anisotropy factor is calculated from the equation $A = 4C_{44}/(C_{11} + C_{33} - 2C_{13})$, and if $A = 1$, the crystal is isotropic while any value smaller or larger than 1 indicates anisotropy. The calculated shear anisotropic factors for the MAX phase compounds are listed in Table 2. The results from Table 2 characterize all the studied MAX phases as being elastically anisotropic. Moreover, Ti_2CdC is considered more anisotropic compared to the other studied compounds. This anisotropy originates from the crystal structure of the studied compounds.

Other important macroscopic properties that depend on the elastic constants are the machinability and ductility [56, 57]. Machinability is defined as the ratio of bulk modulus to C_{44} (B/C_{44}), while ductility is defined as the ratio between bulk modulus and shear modulus, B/G . From Table 3, it is clear that Ti_2CdC possesses the largest value of B/C_{44} and hence more machinable than the rest of the studied MAX phase compounds. The ratio of the bulk modulus (B) to C_{44} may be interpreted as a measure of plasticity [58]. If the values of B/C_{44} are large, it indicate that the material possesses excellent lubricating properties. In terms of the ductility (B/G) [59], it is found that Ti_2PbC and Ti_2CdC are the most ductile material and Ti_2AlC is the least ductile (see Table 3).

3.3 Debye Temperature and Thermal conductivity

The Debye temperature is an important fundamental parameter which is closely related to many physical properties such as specific heat, melting temperatures, thermal conductivity, thermal expansion and lattice vibration. The Debye temperature, θ_D , can be extracted from elastic constants data using by the formula [61],

$$\theta_D = \frac{h}{k_B} \left(\frac{3nN_A\rho}{4\pi M} \right)^{\frac{1}{3}} v_m.$$

Here h is Planck's constant; k_B , Boltzmann's constant; N_A , Avogadro's number; ρ , the density of a material; M , molecular weight; q , the number of atoms in a molecule and v_m , is the averaged sound velocity of the system and is obtained by

$$v_m = \left[\left(\frac{2}{v_t^3} + \frac{2}{v_l^3} \right) / 3 \right]^{-\frac{1}{3}},$$

where v_t and v_l are the longitudinal and transverse sound velocities. v_t and v_l can be determined using the bulk and shear moduli of the materials from the Navier's equations:

$$v_l = \sqrt{\frac{3B + 4G}{3\rho}} \text{ and } v_t = \sqrt{\frac{G}{\rho}},$$

where B , G and ρ are respectively the bulk modulus, shear modulus and the density of the polycrystalline solid. The results for sound velocities, densities and θ_D are summarized in Table 4. A careful look at Table 4, shows that the Ti_2AlN has the highest Debye temperature while Ti_2PbC has the smallest. Higher Debye temperature corresponds to the better thermal conductivity of the compounds. Thus, Ti_2AlN is thermally more conductive in the studied 211 MAX phases. The sound velocities of the considered MAX phases follow the trend: $\text{Ti}_2\text{AlN} < \text{Ti}_2\text{AlC} < \text{Ti}_2\text{GaC} < \text{Ti}_2\text{GaN}$ $\text{Ti}_2\text{SnC} < \text{Ti}_2\text{CdC} < \text{Ti}_2\text{PbC}$. This is expected as the bulk and shear modulus of these materials decrease in the same sequence.

Table 4: The estimated volumic density, ρ , (in g/m^3), sound velocities (v_t , v_l and v_m in km/s) and Debye temperature (θ_D , in K) for Ti_2AlC , Ti_2AlN , Ti_2GaC , Ti_2GaN , Ti_2PbC , Ti_2CdC and Ti_2SnC MAX phases obtained using VASP and QE codes compared with available theoretical and experimental data.

	ρ	v_t	v_l	v_m	θ_D	T_m	Reference
Ti_2AlN	4.12 - 4.28	5229 - 5425	8231 - 8312	5564 - 5747	703 - 747	1574 - 1710	This Calc.
Ti_2AlC	3.87 - 3.99	5096 - 5368	8226 - 8285	5544 - 5616	700 - 727	1548 - 1639	This Calc.
	-	-	-	-	716	-	[19]
Ti_2GaC	5.35 - 5.33	4382 - 4553	6987 - 7327	4817 - 5019	590 - 623	1520 - 1672	This Calc.
Ti_2GaN	5.41 - 5.67	4239 - 4364	7045 - 7272	4683 - 4828	585 - 610	1532 - 1642	This Calc.
	6.03	4506	7552	4988	642	-	LDA [21]
	5.67	4369	7275	4869	610	-	GGA [21]
Ti_2SnC	6.16 - 6.24	3601 - 3861	5980 - 6470	3861 - 3980	473 - 515	1342 - 1545	This Calc.
Ti_2CdC	6.35 - 6.02	3241 - 3286	5615 - 5766	3551 - 3652	422 - 439	1309 - 1413	This Calc.
Ti_2PbC	8.14 - 8.27	2841 - 2991	4922 - 5129	3151 - 3318	369 - 393	1255 - 1391	This Calc.

The melting temperatures (T_m) of hexagonal crystal can be calculated from the elastic constants data by using the empirical formula developed by Fine et al. [60]:

$$T_m = 354 + 1.5(2C_{11} + C_{33}). \quad (1)$$

The calculated melting temperatures of MAX phases is tabulated in Table 4. The high melting temperatures displayed by these MAX phase compounds are encouraging for their application as high temperature structural materials.

Clarke [62] proposed that a material at high temperature possesses a minimum thermal conductivity. The minimum thermal conductivity signifies the theoretical lower limit of intrinsic thermal conductivity of a crystal. It can be calculated from the average sound velocity using [62]:

$$\kappa_{min} = k_B v_m \left(\frac{n N_A \rho}{M} \right), \quad (2)$$

where k_B , v_m , N_A , ρ are respectively, Boltzmann's constant, average sound velocity, Avogadro's constant and density of a crystal. The Clarke's formula [62] is useful in determining the temperature independent minimum thermal conductivity (κ_{min}). The calculated minimum thermal conductivity of 211 MAX phases are tabulated in Table 5. It is clear from Table 5 that the minimum thermal conductivity is directly proportional to the average sound velocity in crystalline solids. As the average sound velocity of Ti_2PbC is lowest, the minimum thermal conductivity of this material is also lowest.

In this study, the lattice thermal conductivities of the MAX phases were estimated using the Slack's model [22] and compared with the available experimental data. Slack's model is most efficient method for determining the lattice thermal conductivity for ceramics like MAX phases. According to Slack's model [22], the temperature dependent lattice thermal conductivity, κ_{ph} of 321 MAX phases can be evaluated using the empirical formula [22]

$$\kappa_{ph} = R \frac{M_{av} \theta_D^3 \delta}{\gamma^2 n^{2/3} T} \quad (3)$$

Here M_{av} is the average atomic weight (in kg/mol) in a molecule, θ_D is the Debye temperature (in K), δ is the cubic root of average atomic volume, n is number of atoms per unit cell, T is the absolute temperature, γ is the Grüneisen parameter derived from Poisson's ratio (ν) and R is a coefficient (in W-mol/kg/m²/K³) depending on γ . The Grüneisen parameter, γ , can be determined as follows [63]:

$$\gamma = \frac{3(1 + \nu)}{2(2 - 3\nu)}. \quad (4)$$

According to Julian [64], the coefficient $R(\gamma)$ can be calculated as:

$$R(\gamma) = \frac{5.720 \times 10^7 \times 0.849}{2 \times (1 - 0.514/\gamma + 0.228/\gamma^2)} \quad (5)$$

Table 5: κ_{min} of Ti_2AlC , Ti_2AlN , Ti_2GaC , Ti_2GaN , Ti_2PbC , Ti_2CdC and Ti_2SnC MAX phases calculated using VASP compared with the available theoretical data.

	Ti_2AlN	Ti_2AlC	Ti_2GaC	Ti_2GaN	Ti_2SnC	Ti_2CdC	Ti_2PbC
κ_{min}	1.41	1.35	1.24	1.18	0.94	0.84	0.73
	-	1.373 [19]	-	-	-	-	-

The obtained results for the lattice thermal conductivities of MAX phases are shown in Figure 2. From our obtained data, it should be noted that the MAX phases which contains Al-atoms have the highest κ_{ph} . This is expected since Al-atom is the lightest as compared to Ga, Cd, Sn and Pb atoms and hence Al scatters less phonons resulting into a higher phonon thermal conductivity. Moreover, the κ_{ph} for Ti_2AlC of 14.6 W/mK obtained at 1300 K is comparable to the one obtained by Chandra et al. (14.71 W/mK) [19] but slightly lower than the experimental value of 16 W/mK [15]. This behaviour is consistent with the results obtained by Chandra et al. [19]. It is also evident from Figure 2 that the estimated κ_{ph} of Ti_2PbC is the lowest among the studied MAX phases. This is expected since Pb is heavier than Al, Ga, Cd and Sn and thus the κ_{ph} of Ti_2PbC should be small as compared to the κ_{ph} of other considered MAX phases.

3.4 Phonon properties

The dynamical property of atoms in the harmonic approximation is obtained by solving eigenvalue problem of dynamical matrix $D(\mathbf{q})$ [65],

$$D(\mathbf{q})\mathbf{e}_{\mathbf{q}j} = \omega^2 \mathbf{e}_{\mathbf{q}j}, \quad (6)$$

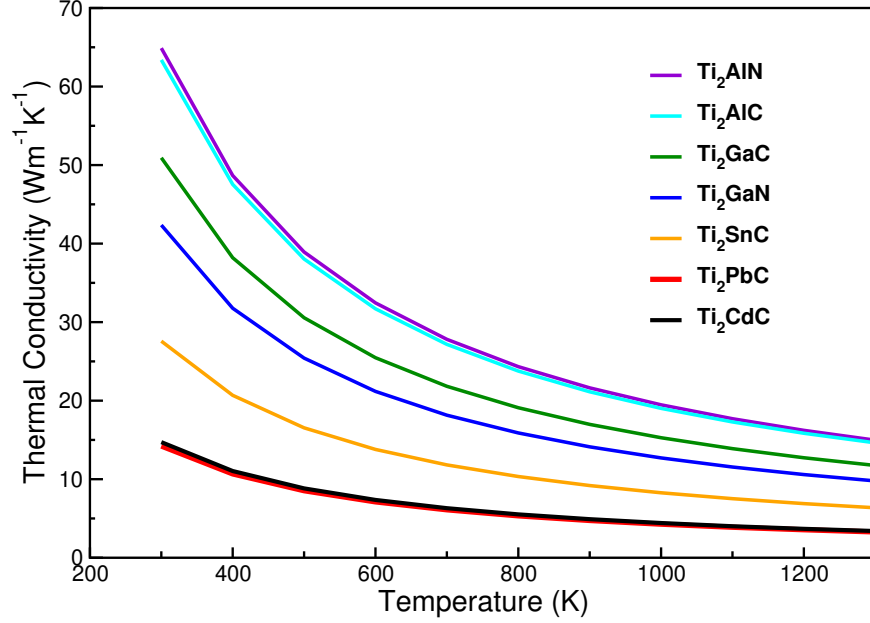
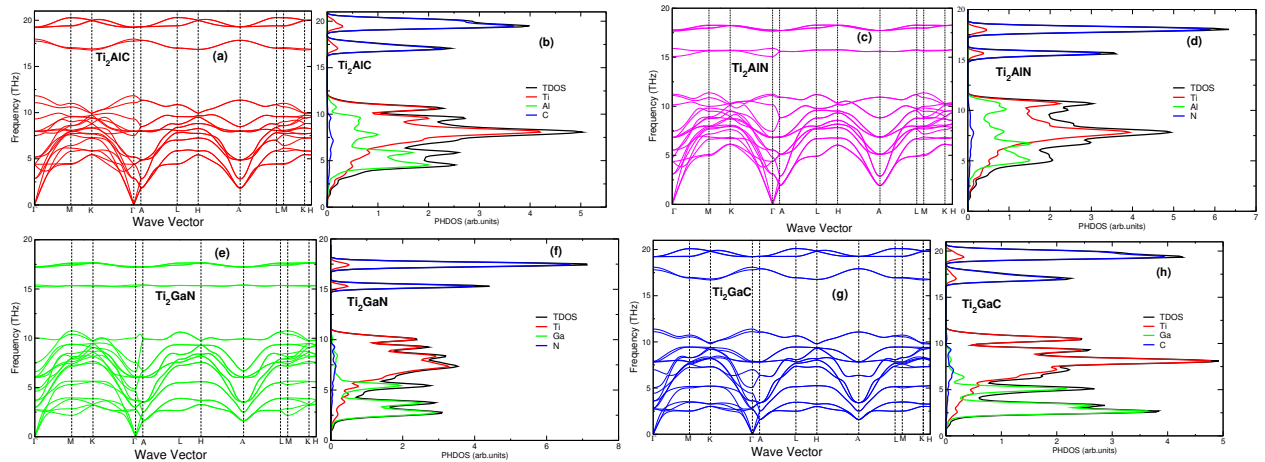


Figure 2: Calculated temperature dependent phonon thermal conductivity for the 211 MAX phases calculated using VASP.

where \mathbf{q} is the wave vector, and j is the band index, $\omega_{\mathbf{q}j}$ and $\mathbf{e}_{\mathbf{q}j}$ are respectively the phonon frequency and polarization vector of the phonon mode labeled by a set $\{\mathbf{q}, j\}$.

The calculated phonon dispersion curves and the phonon density of states (PHDOS) curves along several high symmetry lines in Brillouin zone have been calculated and are shown in Figures 3 (a-n). From Figures 3 (a-n) it is clear that all the phonon frequencies are positive in the Brillouin zone, indicating that the structures of materials under study are dynamically stable. As expected the phonon dispersion curves of the three structures contain 24 phonon modes, including three acoustic and 21 optical branches. The phonon spectra of all the studied materials contain three regions separated by two energy gaps as depicted in Figure 3 (a-n). From the PHDOS [see Figures 3 (a-n)], the acoustic modes of MAX phases are mainly from the vibrations of Al, Ga, Sn, Cd and Pb, the transition metal, Ti, contribute dominantly at low-frequency optical modes while the contribution to the high-frequency optical modes are mainly from the lightest atom i.e N or C-atoms.



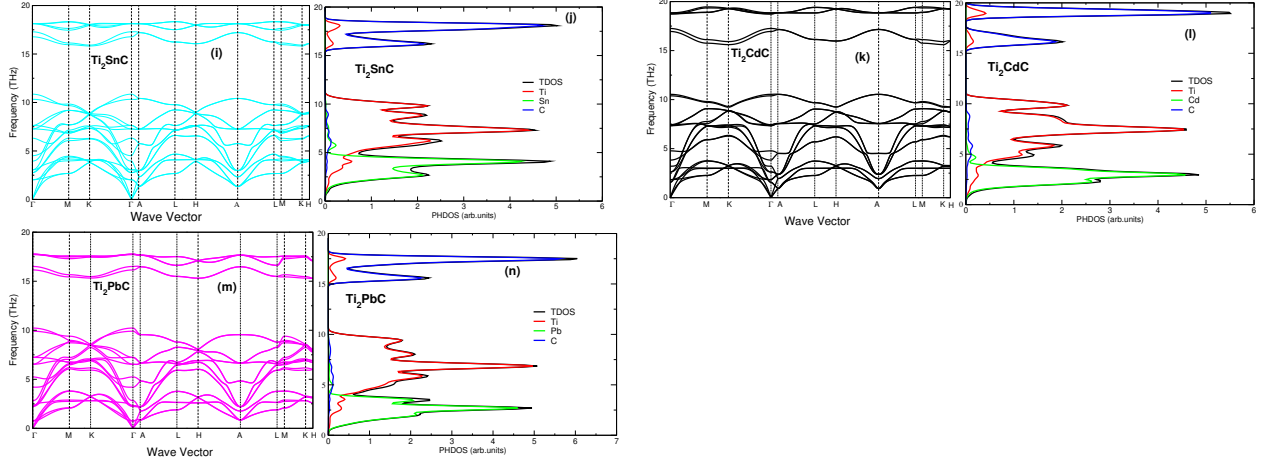


Figure 3: Phonon dispersion curves and phonon density of states (PHDOS) for Ti_2AlC (a, b), Ti_2AlN (c, d), Ti_2GaN (e, f), Ti_2GaC (g, h), Ti_2SnC (i, j), Ti_2CdC (k, l) and Ti_2PbC (m, n) respectively, calculated using VASP.

3.5 Thermodynamic properties

The results of the phonon density of states can be used to calculate the lattice heat capacity (C_v) as function of temperature. The estimated heat capacities at constant volume as functions of temperature are shown in Figures 4 in the temperature range from 0 K to 2000 K. Figure 4 shows that the specific heat, C_v , of all the studied materials follows the Debye model which is proportional to T^3 , as expected [66].

It is clear that at temperature range between 0 and 300 K, heat capacity increases steadily as the temperature increases. It is also found that the Dulong-Petit law is recovered at high temperatures. The difference in C_v is most prominent at lower temperatures as seen in inset Figure 4 (b). From the inset Figure 4 (b), we noted that the trend of the specific heat capacity at constant volume at $T < 250$ K is: $\text{Ti}_2\text{AlN} < \text{Ti}_2\text{AlC} < \text{Ti}_2\text{GaC} < \text{Ti}_2\text{GaN} < \text{Ti}_2\text{SnC} < \text{Ti}_2\text{CdC} < \text{Ti}_2\text{PbC}$.

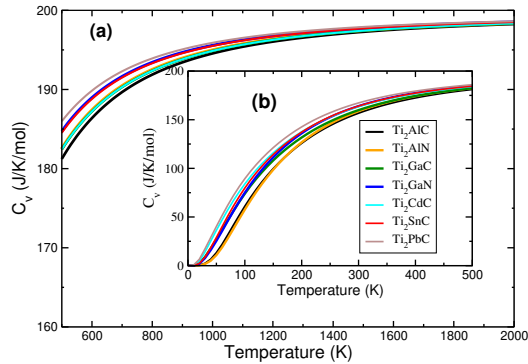


Figure 4: Heat capacities of the MAX phases at temperature range (a) 500 K - 2000 K and (b) 0 - 500 K calculated using VASP.

4 Conclusion

We have investigated the structural, mechanical, lattice dynamics properties as well as the approximate thermal conductivity values of the MAX phases by employing the first-principles DFT calculations using QE and VASP codes. We have calculated the independent elastic constants, bulk modulus, shear modulus, Young's modulus, and elastic anisotropy factor. The compounds are shown to be mechanically stable, elastically anisotropic, and ductile in nature. The calculated elastic constants are found to obey the mechanical stability conditions. The dynamical stability of the MAX compounds are confirmed using phonon dispersion curves. The thermodynamic properties such as specific heat capacity is evaluated using the phonon density of states. We have also calculated the lattice thermal conductivity of studied MAX phases using the Slack's model and found that Ti_2AlN possesses the highest value while Ti_2PbC has the

smallest. The minimum thermal conductivity of these MAX phases have also been estimated using Clarke's formula and show that Ti_2AlN has the highest value of κ_{\min} due to its high value of average sound velocity.

Acknowledgments

We wish to acknowledge support from the Centre for High Performing Computing, South Africa.

Author contribution statement

References

- [1] M. W. Barsoum, *prog. solid state chem.* **28** (2000) 201-81.
- [2] M. W. Barsoum, M. Radovic In: J. K. H. Buschow, R. W. Cahn, M. C. Flemings, B. Hschner, E. J. Kramer, S. Mahajan, P. Reyssier, *Sci. and Tech.* (2004).
- [3] Barsoum MW. *Prog Solid State Chem* 2001;28:201.
- [4] P. Finkel, M. W. Barsoum, T. El-Raghy. *J. Appl. Phys.* **87** (2000) 1701.
- [5] M. W. Barsoum, Germany, Weinheim: Wiley-VCH; (2013).
- [6] p. Eklund, M. Beckers, U. Jansson, H. Högborg, I. Hultman, *Thin Solid Films* **518** (2010) 1851.
- [7] M. Naguib, G. Bentzel, J. Shah, M. W. Barsoum, *Mater Res. Lett.* **2** (2014) 233-240.
- [8] D. Horlait, S. Grasso, A. Chroneos, W. E. Lee. *Mater Res. Lett.* **4** (2016) 137.
- [9] H. Yoo, M. W. Barsoum and T. El-Raghy, *Nature (London)* **407** (2000) 407:581.
- [10] T. El-Raghyet, M. W. Barsoum, *J. Am. Ceram. Soc.* **82** (1999) 2855.
- [11] M. W. Barsoum, *science and technology*. Amsterdam: Elsevier; (2009).
- [12] Ali MA, Ali MS, Uddin MM. *Indian J Pure Appl. Phys.* **54** (2016) 386.
- [13] Gupta S, Hoffman EN, Barsoum MW. *J. Alloys Compd.* **426** (2006) 168-75.
- [14] Manoun B, Saxena SK, Liermann HP, Gulve RP, Hoffman E, Barsoum MW, et al. *Appl. Phys. Lett.* **85** (2004) 1514-6.
- [15] M. W. Barsoum and Sons; MAX phases: properties of machinable ternary carbides and nitrides. Weinheim, Germany: John Wiley and Sons; (2013).
- [16] Y. Medkour, A. Bouhemadou, A. Roumili, *Solid State Commun.* **148** (2008) 459-63.
- [17] X. He, Y. Bai, Y. Li, C. Zhu and M. Li, *Solid State Commun.* **149** (2009) 564-6.
- [18] M. F. Cover, O. Warschkow, M. M. M. Bilek and D. R. McKenzie, *Adv. Eng. Mat.* **10** (2008) 10.
- [19] C. Dhakal et al. *Journal of the European Ceramic Society* **35** (2015) 3203-3212.
- [20] B. Holm, R. Ahuja, S. Li, and B. Johansson, *J. Appl. Phys.* **91** (2002) 9874-9877.
- [21] A. Bouhemadou, *Solid State Sciences* **11** (2009) 1875-1881.
- [22] D. T. Morelli, G. A. Slack. *High lattice thermal conductivity solids. High thermal conductivity materials*. New York, USA: Springer; (2006) 37-68.
- [23] 4. W. Kohn, L.J. Sham, *Phys.Rev.A*, 140 (1965) 1113.
- [24] W. Kohn, L. J. Sham, *Phys. Rev. A* 140 (1965) 113.
- [25] P. Giannozzi, et al., *J.Phys.; Condens. Matter* **21** (2009) 395502.
- [26] S. Baroni, et al. *PWSCF and Phonon: Plane-wave Pseudopotential Codes* (2005) 12297.
- [27] S. Baroni, et al., *Quantum Espresso: Open-source Package for Research in Electronic Structure ; Simulation; and optimization* 12296; <http://www.quantum-espresso.org> 12297;2005
- [28] M. Shishkin, G. Kresse, *Phys. Rev. B* 74 (2006) 035101.
- [29] J. P. Perdew, K. Burke, M. Ernzerhof, *Phys. Rev. Lett.* 77 (1996) 3865.
- [30] G. Kresse and D. Joubert, *Phys. Rev. B* 59 (1999) 1758.
- [31] P. E. Blochl, *Phys. Rev. B* 50 (1994) 17953.

- [32] G Kresse and J Hafner, J. of Phys.: Cond. Matt., 7 (1994) 40.
- [33] H. J. Monkhorst, J. D. Pack, Phys. Rev. B 13 (1976) 5188.
- [34] M. Sundareswari, S. Ramasubramanian and M. Rajagopalan, Solid state communications **150** (2010) 2057-2060.
- [35] M. Born and K. Huang Dynamical Theory of crystal lattices. Clarendon Press, Oxford (1956).
- [36] Y. L. Page, P. Saxe, Phys. Rev. B **65** (2002) 104104.
- [37] A. Togo and I. Tanaka, Scr. Mater. 108 (2015) 1-5.
- [38] Md. Atikur Rahman*, Md. Zahidur Rahaman, American J. of Modern Phys. **4** (2015) 75-91.
- [39] M. Magnuson and M. Mattesini, Thin Solid Films **621** (2017) 108-130.
- [40] H. Vincent, C. Vincent, B. F. Mentzen, S. Pastor and J. Bouix, Mater. Sci. Eng. A, **256** (1998) 83-91.
- [41] M. W. Barsoum, G. Yaroshuk and S. Tyagi, Scr. Mater. **37** (1997) 1583.
- [42] W. Jeitschko, H. Nowotny and F. Benesoky, Monatsh. Chem. **94** (1963) 672.
- [43] W. Jeitschko, H. Nowotny and F. Benesoky, Monatsh. Chem. **95** (1964) 431-435.
- [44] C. Ling, W. B. Tian, P. Zhang, W. Zheng, Y. M. Zhang, Z. M. Sun, J Adv Ceram. **7** (2018) 178-183.
- [45] C. V. L. Anirudh, International journal of emerging technology and advanced engineering (2014).
- [46] O. Beckstein, J. E. Klepeis, G. L. W. Hart and O. Pankratov, Phys. Rev. B **63** (2001) 134112.
- [47] D.C. Wallace, Thermodynamics of Crystals, Wiley, New York, (1972) (Chap. 1).
- [48] F. Birch, Phys. Rev. **71** (1947) 809.
- [49] Y. L. Du, Z. M. Sun, H. Hashimoto and W. B. Tiana, Phys. Lett. A, **372** (2008b) 5220-5223.
- [50] M. F. Cover, O. Warschkow, M. M. Bilek and D. R. McKenzie, J. Phys.: Condens. Matter, **21** (2009) 305403.

- [51] A. Bouhemadou and R. Khenata, J. Appl. Phys. **102** (2007) 043528.
- [52] Y. Bai, X. He, M. Li, Y. Sun, C. Zhu and Y. Li, Solid State Sci. **12** (2010) 144-147.
- [53] R. Hill, Proc. Phys. Soc. **A65** (1952) 349.
- [54] A. Savin, D.C.H. Flad, J. Flad, H. Preuss, H.G. Schnering, Angew. Chem. Int. Ed. **31** (1992) 185-187.
- [55] Z. Sun, S. Li, R. Ahuja, J.M. Schneider, Solid State Commun. **129** (2004) 589.
- [56] Z. Sun, S. F. Pugh, Philosophical magazine **45** (1954), 45,823.
- [57] Z. Sun, D. music, R. Ahuja, J.M.Schneider, Phys. Rev. B **71** (2005), 193402.
- [58] P.A. Vitos, A. Korzhavyi and B. Johansson, Nat. Mater. **2**, (2003) 25-8.
- [59] S. F. Pugh, Philos. Mag. **45** (1954) 823.
- [60] M. E. Fine, L. D. Brown and H.L. Mercus, Scripta Metall. **18** (1984) 951-956.
- [61] D. Music, A. Houben, R. Dronskowski, J. M. Schneider, Phys. Rev. B **75** (2007) 174102.
- [62] D. R. Clarke, Surf. Coat Technol. **163** (2003) 67-74.
- [63] V. N. Belomestnykh, E. P. Tesleva, Technical physics. **8** (2004) 49.
- [64] C. L. Julian, Phys. Rev. **137** (1965) A128.
- [65] J. M. Ziman, Principles of the theory of solids, Cambridge University Press, (1972).
- [66] P. Debye, Zur Theorie der spezifischen Wärmen, Annalen der Physik **39** (1912) 789-839.